REFERENCE: **O3MSAF/KNMI/PUM/004**
ISSUE: 2.2
DATE: 2 May 2017
PAGES: 20

EUMETSAT O3M SAF

The EUMETSAT Network of Satellite Application Facilities

O3M SAF
Ozone and Atmospheric Chemistry Monitoring

PRODUCT USER MANUAL

GOME-2 surface LER product

Product Identifier	Product Name
O3M-89.1	Surface LER from GOME-2 / MetOp-A
O3M-90	Surface LER from GOME-2 / MetOp-B

L.G. Tilstra — Royal Netherlands Meteorological Institute (KNMI)
O.N.E. Tuinder — Royal Netherlands Meteorological Institute (KNMI)
P. Stammes — Royal Netherlands Meteorological Institute (KNMI)

Document status sheet

Issue	Date	Page(s)	Modified Items / Reason for Change
1.0	16-06-2014	all	first version of document
1.1	25-06-2014	all	changes and update after DRR
1.2	13-11-2014	6,7	added sections “Heritage” (1.2) and “Further information” (1.4)
1.3	24-10-2015	8–12	updated section 1.5 ; updated tables 1 and 2
2.0	24-11-2016	all	updated sections 3.1 and 3.2; added section 3.3
2.1	23-02-2017	all	updated sections 1.3, 1.6, 3.1, 3.2 and 4
2.2	02-05-2017	all	changes and update after DRR

Contents

1 Introduction

1.1 Document purpose and scope

This document is the Product User Manual (PUM) for the GOME-2 surface LER products developed at KNMI in the framework of the O3M SAF (Satellite Application Facility on Ozone and Atmospheric Chemistry Monitoring). The aim of this PUM is to present the data format used for the data record, and to explain and describe the contents of the fields contained in the HDF-5 files.

1.2 Heritage

The GOME-2 surface LER product is the Lambertian-equivalent reflectivity (LER) of the Earth's surface observed by the GOME-2 instrument. It is the improved follow-up of earlier surface LER databases based on observations performed by GOME-1 (on the ERS-2 satellite) [*Koelemeijer et al.*, 2003] and OMI (on the Aura satellite) [*Kleipool et al.*, 2008].

The GOME-2 surface LER products are developed at KNMI in the framework of the O3M SAF (Satellite Application Facility on Ozone and Atmospheric Chemistry Monitoring). The algorithm described in the ATBD [*Tilstra et al.*, 2017a] is the direct continuation of the algorithms that were developed by *Koelemeijer et al.* [2003] and *Kleipool et al.* [2008]. Also see *Tilstra et al.* [2017b].

1.3 GOME-2 surface LER products

Two separate GOME-2 surface LER products are produced: one derived from level-1 data from GOME-2 onboard MetOp-A, and one from GOME-2 on MetOp-B. To be more specific:

Product ID	Satellite	Platform	Surface LER versions
O3M-89.1	GOME-2	MetOp-A	MSC & PMD
O3M-90	GOME-2	MetOp-B	MSC & PMD

These GOME-2 surface LER products each contain two surface LER versions: one version based on GOME-2 observations by the Main Science Channels (MSCs) and one version based on GOME-2 observations by the Polarisation Measurement Devices (PMDs). The PMD-based version has the advantage over the MSC-based version that the surface LER is based on eight times as many observations, each with an eight times smaller footprint. This makes the retrieved surface LER less susceptible to residual cloud contamination, statistically more stable, and therefore more reliable. It also allows a higher spatial resolution of the end product, the surface LER database grid.

On the other hand, the surface LER of the PMD-based version is available only for a fixed list of wavelength bands. The wavelengths of the PMD bands are given in Table 5. This limitation is not an issue for the MSC-based surface LER. Here the list of wavelength bands could be determined based on user needs, taking into account that the wavelength bands have to be positioned in the continuum, avoiding strong absorption bands. The selected wavelength bands are given in Table 4.

1.4 Database versions

Table 1 provides an overview of the database versions that have been produced.

Version number	O3M SAF release	MetOp-A	MetOp-B	Description ; Comments
1.0		+		first version ; created for testing purposes only
1.1	Yes	+		version released by the O3M SAF after review ; Product ID: O3M-89 ; various improvements were implemented after the initial testing phase
1.2		+		improved handling of residual clouds ; improved handling of missing data (due to polar night)
1.3		+		improved detection of cloud contamination ; improved handling of missing data (due to polar night) ; minor change to the data format
1.4		+		ozone taken from L2 product instead of assimilated fields ; better treatment of missing data via snow/ice constraint on potential donor cells
1.5		+		improved error calculation (uncertainty field)
1.6		+		further fine-tuned treatment of missing data
1.7		+		switched to 32-bits floats and applied h5repack
2.0		+	+	higher spatial resolution near coastlines ; minor changes to the data format
2.1	Yes	+	+	version released by the O3M SAF after review ; Product IDs: O3M-89.1 and O3M-90 (MetOp-A and MetOp-B, respectively)

Table 1: Overview of the database versions that were produced. Only versions 1.1 and 2.1 have been officially released by the O3M SAF. A MetOp-B database was first introduced for data version 2.1.

1.5 Further information

1.5.1 The O3M SAF website

Further up-to-date information and documentation on the GOME-2 surface LER products are available on the O3M SAF website: http://o3msaf.fmi.fi

Note: As of 1 March 2017, the O3M SAF has changed its name into Satellite Application Facility on Ozone and Atmospheric Chemistry Monitoring (AC SAF). The AC SAF website is: http://acsaf.org

Requests for data and questions with regards to O3M SAF products should be directed to the user services. Contact information is also available on the website mentioned above.

1.5.2 Acknowledgement instructions

When O3M SAF data are used for operational or scientific purposes, the source of these data should be acknowledged. For example: "The data of the GOME-2 Lambertian-equivalent reflectivity (LER) are provided by KNMI in the framework of the EUMETSAT Satellite Application Facility on Ozone and Atmospheric Chemistry Monitoring (O3M SAF)".

1.6 Suggested reading material

Herman, J. R., and E. A. Celarier (1997), Earth surface reflectivity climatology at 340–380 nm from TOMS data, *J. Geophys. Res., 102*(D23), 28,003–28,011, doi:10.1029/97JD02074.

Koelemeijer, R. B. A., J. F. de Haan, and P. Stammes (2003), A database of spectral surface reflectivity in the range 335–772 nm derived from 5.5 years of GOME observations, *J. Geophys. Res., 108*(D2), 4070, doi:10.1029/2002JD002429.

Kleipool, Q. L., M. R. Dobber, J. F. de Haan, and P. F. Levelt (2008), Earth surface reflectance climatology from 3 years of OMI data, *J. Geophys. Res., 113*, D18308, doi:10.1029/2008JD010290.

Popp, C., P. Wang, D. Brunner, P. Stammes, Y. Zhou, and M. Grzegorski (2011), MERIS albedo climatology for FRESCO+ O2 A-band cloud retrieval, *Atmos. Meas. Tech., 4*, 463–483, doi:10.5194/amt-4-463-2011.

Tilstra, L. G., O. N. E. Tuinder, P. Wang, and P. Stammes (2017), Surface reflectivity climatologies from UV to NIR determined from Earth observations by GOME-2 and SCIAMACHY, *J. Geophys. Res. Atmos., 122*, doi:10.1002/2016JD025940.

1.7 Abbreviations and acronyms

AAI	Absorbing Aerosol Index
AAH	Absorbing Aerosol Height
ATBD	Algorithm Theoretical Basis Document
BRDF	Bidirectional Reflectance Distribution Function
BSA	Black-Sky Albedo
CDOP	Continuous Development & Operations Phase
DAK	Doubling-Adding KNMI
DU	Dobson Units, 2.69×10^{16} molecules cm^{-2}
EUMETSAT	European Organisation for the Exploitation of Meteorological Satellites
ENVISAT	Environmental Satellite
ERS	European Remote Sensing Satellite
ESA	European Space Agency
ETOPO-4	Topographic & Bathymetric data set from the NGDC, 4 arc-min. resolution
FOV	Field-of-View
FRESCO	Fast Retrieval Scheme for Cloud Observables
FWHM	Full Width at Half Maximum
GOME	Global Ozone Monitoring Experiment
HDF	Hierarchical Data Format
IT	Integration Time
KNMI	Koninklijk Nederlands Meteorologisch Instituut (De Bilt, NL)
LER	Lambertian-Equivalent Reflectivity
LUT	Look-Up Table
MERIS	Medium Resolution Imaging Spectrometer
METOP	Meteorological Operational Satellite
MLS	Mid-Latitude Summer
MSC	Main Science Channel
NISE	Near-real-time Ice and Snow Extent
NOAA	National Oceanic and Atmospheric Administration
NGDC	NOAA's National Geophysical Data Center (Boulder, Colorado, USA)
NRT	Near-Real-Time
OMI	Ozone Monitoring Instrument
O3M SAF	Satellite Application Facility on Ozone and Atmospheric Chemistry Monitoring
PMD	Polarisation Measurement Device
PSD	Product Specification Document
PUM	Product User Manual

RTM	Radiative Transfer Model
SCIAMACHY	Scanning Imaging Absorption Spectrometer for Atmospheric Chartography
SZA	Solar Zenith Angle
TEMIS	Tropospheric Emission Monitoring Internet Service
TOA	Top-of-Atmosphere
TOMS	Total Ozone Mapping Spectrometer
UTC	Universal Time Co-ordinate
UV	Ultra-Violet
VIS	Visible
VR	Validation Report
VZA	Viewing Zenith Angle

2 Surface reflectivity databases for the UV-VIS

2.1 Introduction

Surface reflectivity databases are needed for cloud, aerosol and trace gas retrievals. One of the first surface reflectivity databases retrieved using UV satellite remote sensing techniques is the Total Ozone Mapping Spectrometer (TOMS) [*Heath et al.*, 1975] surface LER database [*Herman and Celarier*, 1997]. The retrieved reflectivity is the Lambertian-equivalent reflectivity (LER) of the surface found from scenes which are assumed to be cloud free. The retrieval method relies on the removal of the (modelled) atmospheric contribution from the (observed) top-of-atmosphere (TOA) reflectance. In this approach the surface is defined to behave as a Lambertian reflector. The TOMS surface LER database ($1.25^\circ \times 1^\circ$) was retrieved for 340 and 380 nm only, which limits its usefulness.

The GOME [*Burrows et al.*, 1999] surface reflectivity database provides the surface LER on a $1^\circ \times 1^\circ$ grid for 11 wavelength bands between 335 and 772 nm [*Koelemeijer et al.*, 2003]. Although this is already quite an improvement with respect to the TOMS surface LER database, the database is still limited in quality by the low number of measurements from which the surface LER had to be extracted and the large GOME footprint size (see Table 3). In particular, pixels over sea are often affected by residual cloud contamination. In these cases the surface LER was retrieved from scenes which were not sufficiently cloud free. In other cases, e.g. snow surfaces, the surface LER was retrieved from a few measurements which were not representative for the entire month.

A large improvement on these points is the OMI surface reflectivity database [*Kleipool et al.*, 2008]. First, the OMI instrument [*Levelt et al.*, 2006] has a much smaller footprint size (24×13 km^2 at nadir) combined with a larger global coverage (see Table 3). This leads to better statistics and results in a higher accuracy for the surface LER retrieval. Second, the higher number of measurements allows for inspecting the distribution of scene LERs for each grid cell, and for making a more sophisticated selection of representative (cloud-free) scenes instead of directly taking the minimum scene LER value like in the case of the TOMS and GOME databases. Third, the provided OMI surface LER database has a higher spatial resolution ($0.5^\circ \times 0.5^\circ$ grid). The limiting factor is the OMI wavelength range. The longest wavelength in the OMI surface LER database is 499 nm.

The GOME-2 series of satellite instruments does not have some of the limitations of the satellite instruments mentioned above and can be used to create a better, more reliable surface LER database [*Tilstra et al.*, 2017b]. To be more specific, it has the spectral range of GOME but a much smaller footprint (80×40 km^2) which is constant over the full swath width. Additionally, the number of measurements that are available per longitude/latitude cell is smaller than that of OMI, but enough to perform a statistical analysis on the distribution of retrieved scene LERs. Developing the GOME-2 surface LER retrieval the approach used for the OMI surface LER database was followed.

The main advantage of the GOME-2 surface LER database with respect to the OMI surface LER database is the wider wavelength range of the GOME-2 instrument. Additionally, the retrieval algorithm uses aerosol information, available via the GOME-2 Absorbing Aerosol Index (AAI) product, to filter out scenes with large aerosol loadings, as these scenes can result in inaccurate values of the retrieved surface LER. This filtering is especially important for locations over desert areas.

2.2 Tables

In Table 3 we summarise the properties of the discussed surface reflectivity databases. For GOME-2 we provide the specifications for the MSC-based and PMD-based algorithms. In Table 4 we list the wavelength bands of the surface reflectivity databases, and their application. In Table 5 we provide the wavelengths of the GOME-2 PMD bands, relevant to the PMD-based algorithm. The selection of the wavelength bands for the GOME-2 MSC-LER was influenced largely by the already existing surface LER databases. Below 325 nm the surface contribution to the TOA reflectance is low, which prevents an accurate retrieval of the surface LER below this wavelength. For the GOME-2 PMD-LER this means that the surface LER for PMD 1 and 2 cannot be retrieved, as indicated.

instrument	TOMS	GOME	OMI	MSC - GOME-2 - PMD	
satellite	Nimbus-7	ERS-2	Aura	MetOp-A/B	
equator crossing time (LT)	12:00	10:30	13:45	09:30	
dayside flight direction	S→N	N→S	S→N	N→S	
number of days for global coverage	1	3	1	1.5	
pixel size at nadir (km × km)	50 × 50	320 × 40	24 × 13	80 × 40	10 × 40
number of usable pixels per orbit	∼12000	∼1300	∼83000	∼11000	∼88000
dataset time range (*)	1978–1993	1995–2000	2004–2007	2007→ (*)	2008→ (*)
selected wavelength bands	2	11	23	21	13
wavelength range covered (nm)	340–380	335–772	328–499	335–772	335–799
band width (nm)	1.0	1.0	1.0	1.0	see text
spatial resolution (°lon × °lat)	1.25 × 1.0	1.0 × 1.0	0.5 × 0.5	1.0 × 1.0	0.5 × 0.5
reference	HC1997	KHS2003	KDHL2008	TTWS2017	

Table 3: Characteristics and properties of the UV-VIS surface LER databases, and of the satellite instruments from which they are derived. Wavelength band information can be found in Tables 4/5.

(*)The longer the time period covered, the higher the number of times a certain region has been observed. This increases the chances of having observed this region under clear sky conditions. Occasional reprocessing over longer time periods therefore increases the quality, stability, and reliability of the surface LER product. GOME-2 data are available from January 2007 (MetOp-A). GOME-2 data from MetOp-B are available since December 2012.

λ (nm)	TOMS	GOME	OMI	GOME-2	application / relevance
328			+		LER, ozone, HCHO
335		+	+	+	LER, ozone, HCHO
340	+			+	LER, aerosol, HCHO, BrO
342			+		LER, aerosol, HCHO, BrO
345			+		LER, aerosol, HCHO, BrO
354			+	+	LER, aerosol, HCHO, BrO, OClO
367			+	+	LER, aerosol, OClO
372			+		LER, aerosol, OClO
376			+		LER, aerosol, OClO
380	+	+	+	+	LER, aerosol, OClO
388			+	+	LER, aerosol, OClO
406			+		LER, aerosol
416		+	+	+	LER, aerosol
418			+		LER, aerosol
425			+	+	LER, aerosol, NO_2
440		+	+	+	LER, aerosol, NO_2
442			+		LER, aerosol, NO_2
452			+		LER, aerosol, NO_2
463		+	+	+	LER, aerosol, NO_2, O_2-O_2
471			+		LER, aerosol, NO_2, O_2-O_2
477			+		LER, aerosol, NO_2, O_2-O_2
488			+		LER, aerosol, NO_2, O_2-O_2
494		+	+	+	LER, aerosol, NO_2
499			+		LER, aerosol
510				+	LER, aerosol
526				+	LER, aerosol, vegetation
546				+	LER, aerosol, vegetation
555		+		+	LER, aerosol, vegetation
564				+	LER, aerosol, vegetation
610		+		+	LER, aerosol, H_2O
640				+	LER, aerosol, H_2O
670		+		+	LER, aerosol, H_2O, O_2-B
758		+		+	LER, aerosol, O_2-A
772		+		+	LER, aerosol, O_2-A
Total:	2	11	23	21	

Table 4: Wavelength bands of the four monochromatic surface LER databases, and their applications. All wavelength bands are located outside strong gaseous absorption bands in order to avoid complicated modelling of the radiative transfer. The number of wavelength bands is also given.

PMD	λ (nm)	application / relevance	PMD	λ (nm)	application / relevance
01	312	not retrieved	09	460	LER, aerosol, NO_2, O_2-O_2
02	317	not retrieved	10	519	LER, aerosol
03	325	LER, ozone, HCHO, SO_2	11	554	LER, aerosol
04	332	LER, ozone, HCHO	12	589	LER, aerosol
05	338	LER, aerosol, HCHO, BrO	13	639	LER, aerosol, H_2O
06	369	LER, aerosol, OClO	14	756	affected by O_2 absorption
07	382	LER, aerosol, OClO	15	799	LER, aerosol
08	413	LER, aerosol			

Table 5: Wavelength information for the PMD bands used in the PMD-based surface LER algorithm. The wavelength definition follows PMD band definition v3.1, so the list applies to MetOp-A PMD data from after 11 March 2008 as well as to all MetOp-B PMD data.

The widths of the PMD bands are not provided in Table 5, but these (and other information) can be found in the "GOME-2 Factsheet" [*EUMETSAT*, 2015]. For some of the PMD bands the relatively broad wavelength range covered leads to inference with absorption bands. For instance, PMD 14 overlaps with the oxygen-A absorption band and this has affected the retrieved surface LER.

3 The GOME-2 surface LER product

3.1 Product files

For each of the two GOME-2 surface LER data records (determined for MetOp-A and MetOp-B as explained in section 1.3) the MSC and PMD surface LER databases are separated into individual files. The GOME-2 surface LER product therefore consists of two files per instrument, e.g.:

`GOME-2_MetOp-B_MSC_025x025_surface_LER_v2.1.hdf5` (609 Mb)
`GOME-2_MetOp-B_PMD_025x025_surface_LER_v2.1.hdf5` (652 Mb)

The format of the GOME-2 surface LER product files is HDF-5. The fields contained in the product files are presented in Table 6 and are discussed in section 3.2.

3.2 Contents of the product files

The parameter *Period* is a string that lists the years of data which were used for the retrieval of the surface LER. The *Wavelength* field is an array listing the centre wavelengths of each of the wavelength or PMD bands. The width of the wavelength bands is 1.0 nm for the MSC-LER. For the PMD-LER, this width is by definition the width of the PMD band in question. More information about the PMD bands can be found in the "GOME-2 Factsheet" [*EUMETSAT*, 2015]. The number of wavelength bands (nwav) is either 21 (MSC-LER) or 13 (PMD-LER). The *Longitude* and *Latitude* arrays contain the centre longitudes or latitudes of the various grids contained in the product. The dimensions of the grids are defined by nlon=1440, nlat=720 for both the MSC-LER and the PMD-LER.

data set name	**data type**	**units**	**description**
Period	string	–	years covered, e.g., "2007–2013"
Wavelength	float(nwav)	nm	wavelengths of the wavelength bands
Longitude	float(nlon)	degrees	centre longitude of row
Latitude	float(nlat)	degrees	centre latitude of column
Minimum_LER	float(nmon,nwav,nlon,nlat)	–	"MIN-LER" surface LER
Mode_LER	float(nmon,nwav,nlon,nlat)	–	"MODE-LER"surface LER
Uncertainty	float(nmon,nwav,nlon,nlat)	–	estimated uncertainty in MODE-LER
Flag	integer(nmon,nlon,nlat)	–	quality flag (0,1,2,3,4,5)

Table 6: Fields contained in the GOME-2 surface LER products. MSC-LER: nwav=21, nlon=1440, nlat=720; PMD-LER: nwav=13, nlon=1440, nlat=720. The number of months (nmon) is 12.

The *Minimum_LER* and *Mode_LER* fields hold the surface LER grids retrieved using the MIN-LER and MODE-LER approaches. As explained in the ATBD, the MIN-LER approach determines the surface LER in the traditional way in which the minimum scene LER that is found over time for a certain location is assumed to be representative for the surface LER. The MODE-LER approach analyses the distribution of retrieved scene LERs and, depending on the characteristics of the distribution and on the surface type, takes the mode or the mimimum of the distribution. Over sea surfaces it always takes the minimum. Therefore, in most cases, the MODE-LER algorithm is identical to the MIN-LER algorithm. Nevertheless, there are differences over desert areas and snow/ice surfaces.

The two approaches are explained more extensively in the ATBD. It is up to the user to decide which of the two surface LER grids suits best. Both are separately validated in the Validation Report. An estimated uncertainty for the surface LER is provided in the *Uncertainty* field. Note that this *Uncertainty* field is calculated for (and from) the *Mode_LER* field. The three types of grids described above are comprised of nmon $\times$ nwav $\times$ nlon $\times$ nlat values, where the number nmon=12 refers to the twelve calendar months. For the MSC-LER we have have the dimensions set to nwav=21, nlon=1440, nlat=720. For the PMD-LER the dimensions are nwav=13, nlon=1440, nlat=720.

An integer quality flag is provided in the field *Flag*. The dimension of the matrix is 12 $\times$ nlon $\times$ nlat. Possible values range from 0 to 5. Table 7 explains the meaning of these flags. This table was taken directly from the ATBD. The ATBD provides a more complete description of the quality flag.

Flag	Meaning of flag
0	data are ok; no corrections applied
1	residual cloud contamination above ocean detected – replaced by nearby cloud-free cell
2	residual cloud contamination above ocean detected – no suitable replacement could be found (the pixel remains cloud contaminated or receives the LER spectrum of a non-representative donor cell)
3	missing data for polar regions which are observed only part of the year – filled in using nearest month with reliable surface LER data
4	missing data throughout the entire year
5	suspect surface LER value retrieved for at least one of the wavelengths

Table 7: Definition of the quality flags that are provided along with the surface LER products.

3.3 Intrinsic spatial resolution

The resolution of the grids provided in the surface LER products is $0.25° \times 0.25°$, for both the MSC-LER and the PMD-LER. The *intrinsic* resolution, however, is different. For the MSC-LER,

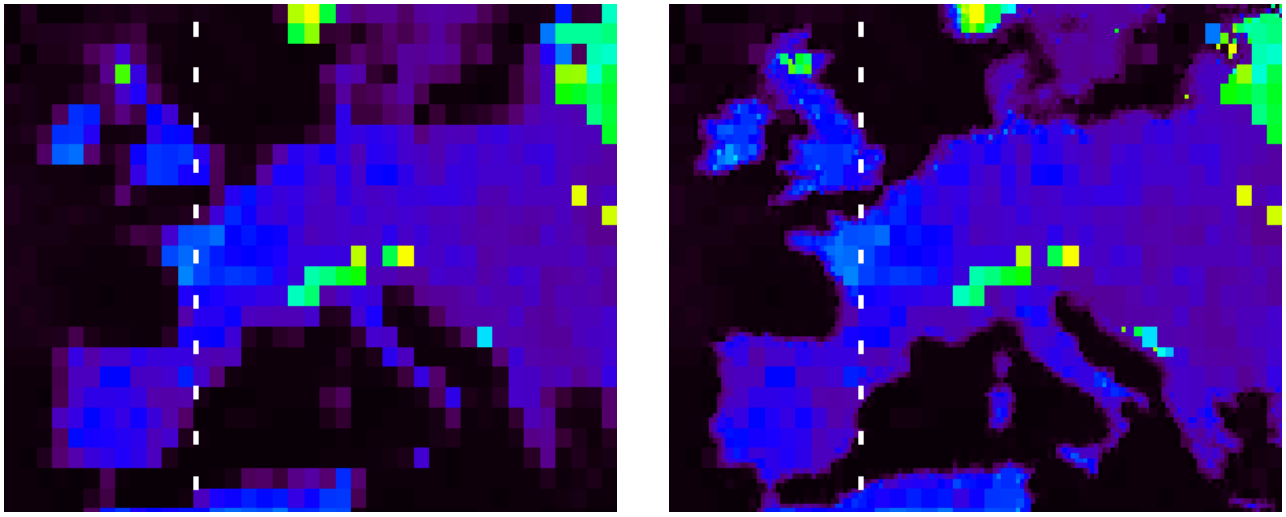

Figure 1: Surface LER retrieved at 772 nm, for the month March and presented for western Europe. Left: original one-degree resolution; Right: increased resolution of 0.25-degrees near the coast.

the intrinsic resolution is $1^\circ \times 1^\circ$ for non-coastal areas. For the coastal areas, the intrinsic resolution switches to $0.5^\circ \times 0.5^\circ$ near the coastline, and to $0.25^\circ \times 0.25^\circ$ at the coastline. See Figure 1. This is done to achieve an important higher spatial resolution at the coastline. At the same time we do not want to compromise the quality of the grid cells that do not contain a coastal area.

Therefore, the intrinsic spatial resolution of the MSC-LER is $1^\circ \times 1^\circ$, except for the coastline, where the intrinsic resolution is $0.25^\circ \times 0.25^\circ$. For the PMD-LER, the intrinsic spatial resolution for non-coastal areas is $0.5^\circ \times 0.5^\circ$, and $0.25^\circ \times 0.25^\circ$ at the coastline. The intrinsic resolution of the PMD-LER is therefore higher than that of the MSC-LER, even though the size of their grids is identical. The method that is used to control the intrinsic spatial resolution is explained in the ATBD.

It is important for users of the GOME-2 surface LER databases to realise that the increased resolution of the database grid (by a factor of 4×4 for the MSC-LER and by a factor of 2×2 for the PMD-LER) was needed to accommodate the higher resolution near the coastline, and that the real intrinsic resolution in other areas is the same as it was for the previous version of the database. However, because of the larger amount of (smaller) grid cells in the database, the various methods of users to link the database grid cells to the measurements footprints of their observations may actually lead to small changes. Such changes can occur everywhere, not only near the coastlines. The users should check how their retrieval codes deal with the higher resolution of the new database grids.

3.4 User guideline

Users that need to use surface albedo input for their retrievals based on GOME-2A data should use the GOME-2A surface LER database. Likewise, users that work with GOME-2B data should make

use of the GOME-2B surface LER database. Doing this makes most sense as radiometric calibration issues that are specific to the individual instruments are likely to cancel out this way.

Users that need surface albedo input but are not using GOME-2 data for their retrievals should probably use the GOME-2A surface LER database. The GOME-2A surface LER database is based on 7 years of data, while the GOME-2B database is based on only 4 years of data. The GOME-2A database therefore has a slightly higher quality than the GOME-2B database.

More details and background information can be found in *Tilstra et al.* [2017b].

4 Product quality

The validation approach and the methods that were used to get to the results are described extensively in *Tilstra et al.* [2017b]. A report on the most current product quality can be found in the Validation Report [*Tilstra et al.*, 2017c]. For the GOME-2A and GOME-2B databases, the results presented in this VR indicate that the GOME-2A and GOME-2B MSC MIN-LER and MODE-LER surface LER products are in general accurate within 0.01 over the ocean and accurate within 0.04 over snow/ice surfaces. These numbers were derived on the basis of comparisons of the GOME-2A surface LER database with the GOME-1 and OMI surface LER databases, combined with intercomparison between the GOME-2A and GOME-2B surface LER databases. A very good agreement is found between the GOME-2A and GOME-2B MSC surface LER databases.

For the PMD-LER databases, the results that were found are similar but a bias of -0.01 is present in the GOME-2A PMD-LER, presumably related to calibration issues of the PMDs. The intercomparison between the PMD-LER of GOME-2A and GOME-2B showed that the GOME-2B PMD-LER is a bit higher for the shorther wavelengths. It is actually closer to the MSC-LER surface LER products, suggesting that the calibration of the PMD-bands is a bit better than that of GOME-2A. All in all, the GOME-2A and GOME-2B PMD-LER databases perform well.

For the individual locations (cells) in the database, an uncertainty field is present in the database. This uncertainty field presents for each month of the year, for each wavelength band, and for each cell in the latitude/longitude grid, an estimation of the uncertainty in the retrieved surface LER.

References

Burrows, J. P., et al. (1999), The Global Ozone Monitoring Experiment (GOME): Mission concept and first scientific results, *J. Atmos. Sci., 56*(2), 151–175.

EUMETSAT (2015), GOME-2 Factsheet, Doc. No. EUM/OPS/DOC/10/1299, Issue 4b, 17 March 2015, EUMETSAT, Darmstadt, Germany.

Heath, D. F., A. J. Krueger, H. A. Roeder, and B. D. Henderson (1975), The Solar Backscatter Ultraviolet and Total Ozone Mapping Spectrometer (SBUV/TOMS) for NIMBUS G, *Opt. Eng., 14*(4), 144323, doi:10.1117/12.7971839.

Herman, J. R., and E. A. Celarier (1997), Earth surface reflectivity climatology at 340–380 nm from TOMS data, *J. Geophys. Res., 102*(D23), 28,003–28,011, doi:10.1029/97JD02074.

Kleipool, Q. L., M. R. Dobber, J. F. de Haan, and P. F. Levelt (2008), Earth surface reflectance climatology from 3 years of OMI data, *J. Geophys. Res., 113*, D18308, doi:10.1029/2008JD010290.

Koelemeijer, R. B. A., J. F. de Haan, and P. Stammes (2003), A database of spectral surface reflectivity in the range 335–772 nm derived from 5.5 years of GOME observations, *J. Geophys. Res., 108*(D2), 4070, doi:10.1029/2002JD002429.

Levelt, P. F., G. H. J. van den Oord, M. R. Dobber, A. Mälkki, H. Visser, J. de Vries, P. Stammes, J.O.V. Lundell, and H. Saari (2006), The Ozone Monitoring Instrument, *IEEE Trans. Geosci. Remote Sens., 44*(5), 1093–1101, doi:10.1109/TGRS.2006.872333.

Popp, C., P. Wang, D. Brunner, P. Stammes, Y. Zhou, and M. Grzegorski (2011), MERIS albedo climatology for FRESCO+ O2 A-band cloud retrieval, *Atmos. Meas. Tech., 4*, 463–483, doi:10.5194/amt-4-463-2011.

Tilstra, L. G., O. N. E. Tuinder, and P. Stammes (2017a), GOME-2 surface LER product – Algorithm Theoretical Basis Document, *KNMI Report O3MSAF/KNMI/ATBD/003*, Issue 2.2, May 2, 2017.

Tilstra, L. G., O. N. E. Tuinder, P. Wang, and P. Stammes (2017b), Surface reflectivity climatologies from UV to NIR determined from Earth observations by GOME-2 and SCIAMACHY, *J. Geophys. Res. Atmos., 122*, doi:10.1002/2016JD025940.

Tilstra, L. G., O. N. E. Tuinder, and P. Stammes (2017c), GOME-2 surface LER product – Validation Report, *KNMI Report SAF/O3M/KNMI/VR/002*, Issue 2/2017, May 2, 2017.